J|A|C|S
ARTICLES
Published on Web 03/22/2002

Low-Temperature Photosensitized Oxidation of a Guanosine Derivative and Formation of an Imidazole Ring-Opened Product

Chimin Sheu,† Ping Kang, Saeed Khan,‡ and Christopher S. Foote*

Contribution from the Department of Chemistry and Biochemistry, University of California, Los Angeles, Los Angeles, California 90095-1569

Received July 11, 2001. Revised Manuscript Received January 7, 2002

Abstract: An organic-soluble guanosine derivative, 2′,3′,5′-*O*-(*tert*-butyldimethylsilyl)guanosine (**1**), was prepared and its photosensitized oxidation was carried out in several solvents at various temperatures. Singlet oxygen is the reactive oxidizing agent responsible for this reaction. Neither an endoperoxide nor a dioxetane intermediate was detected by low-temperature NMR even at −78 °C. A product (**A**) with an oxidized imidazole ring was the only major product detected at room temperature; this compound could be isolated by low-temperature column chromatography and was characterized by ^{1}H and ^{13}C and mass spectroscopy. CO_2 was the other major product. A small amount of the corresponding 8-oxo-7,8-dihydroguanosine derivative **B** was detected during the initial stage of the photooxidation and was shown to be intermediate in the formation of two products of extensive degradation, **C** and **D**. Reaction of **1** with the singlet oxygen analogues 4-methyl-1,2,4-triazoline-3,5-dione (MTAD) and 4-phenyl-1,2,4-triazoline-3,5-dione (PTAD) gave products consistent with a proposed mechanism involving the rearrangement of an initially formed endoperoxide to give **A** and **B** from reaction of **1** with singlet oxygen.

Introduction

Photodynamic action is the general term for the effects induced within organisms and cells, and on biologically important molecules by visible light in the presence of molecular oxygen and photosensitizing dyes. Recently, photodynamic therapy (PDT) has been used to produce remission of a number of different types of malignant tumors and treatment of some viral diseases.[1−7] Harmful photodynamic effects have been reported to occur in many kinds of biological systems. Several key types of biomolecules, such as nucleic acids,[8−11] membrane lipids,[12−15] and proteins,[16−20] are sites of these deleterious effects on living systems. The biological effects caused by this action have been extensively studied and it is now generally accepted that the damage is due to photooxidative destruction or modifications of vital biomolecules.[8,9,21−23] Among these modifications, oxidative damage to cellular DNA is of particular interest.[10]

The relative reactivity of nucleic acid components toward reactive oxygen species such as superoxide, hydrogen peroxide, and hydroxyl radical has been extensively studied. Superoxide generated by radiolysis has little effect on nucleosides,[24] and the rate of superoxide decomposition is not affected by the presence of DNA.[25] Hydrogen peroxide resulting both from radiolytic processes[26] and the disproportion between $O_2^{\bullet-}$ and

* Address correspondence to this author. E-mail: foote@chem.ucla.edu.
† Current address: Macronix International, 3, Creation Road, Science Industrial Based Park, Hsinchu, Taiwan, ROC.
‡ To whom X-ray correspondence should be addressed.

(1) Dougherty, T. J. In *Porphyrin Localization and Treatment of Tumors*; Doiron, D. R., Gomer, C. J., Eds.; Alan R. Liss: New York, 1984; Progress in Clinical and Biological Research, Vol. 170, pp 75−87.
(2) Dougherty, T. J. In *Advances in Photochemistry*; Volman, D. H., Hammond, G. S., Neckers, D. C., Eds.; John Wiley & Sons: New York, 1992; Vol. 17, pp 275−311.
(3) Marcus, S. L. In *Photodynamic Therapy*; Henderson, B. W., Dougherty, T. J., Eds.; Marcel Dekker: New York, 1992; pp 219−258.
(4) Foote, C. S. In *Porphyrin Localization and Treatment of Tumors*; Doiron, D. G., Gomer, C. J., Eds.; Alan R. Liss, Inc.: New York, 1984; pp 3−18.
(5) Phillip, M. J.; McMahon, J. D.; O'Hara, M. D.; Hetzel, F. W.; Amsterdamsky, C.; Schaap, A. P. In *Porphyrin Localization and Treatment of Tumors*; Doiron, D. R., Gomer, C. J., Eds.; Alan R. Liss: New York, 1984; Vol. Progress in Clinical and Biological Research Volume 170, pp 563−570.
(6) Curnow, A.; Haller, J. C.; Bown, S. G. *J. Photochem. Photobiol. B−Biol.* **2000**, *58*, 149−155.
(7) De Rosa, F. S.; Bentley, M. *Pharm. Res.* **2000**, *17*, 1447−1455.
(8) Cadet, J.; Vigny, P. In *Bioorganic Photochemistry*; Morrison, H., Ed.; John Wiley & Sons: New York, 1990; Vol. 1, pp 1−272.
(9) Foote, C. S. In *Oxygen and Oxy-radicals In Chemistry and Biology*; Rodgers, M. A. J., Powers, E. L., Eds.; Academic Press: New York, 1981; pp 425−440.
(10) Ravanat, J. L.; Di Mascio, P.; Martinez, G. R.; Medeiros, M. H. G.; Cadet, J. *J. Biol. Chem.* **2000**, *275*, 40601−40604.
(11) Schulz, I.; Mahler, H. C.; Boiteux, S.; Epe, B. *Mutat. Res.-DNA Repair* **2000**, *461*, 145−156.
(12) Bachowski, G. J.; Morehouse, K. M.; Girotti, A. W. *Photochem. Photobiol.* **1988**, *47*, 635−645.
(13) Santus, R.; Reyftmann, J.-P. *Biochimie* **1986**, *68*, 843−848.
(14) Bocking, T.; Barrow, K. D.; Netting, A. G.; Chilcott, T. C.; Coster, H. G. L.; Hofer, M. *Eur. J. Biochem.* **2000**, *267*, 1607−1618.
(15) Korytowski, W.; Girotti, A. W. *Photochem. Photobiol.* **1999**, *70*, 484−489.
(16) Balasubramanian, D.; Du, X.; Zigler, J. S., Jr. *Photochem. Photobiol.* **1990**, *52*, 761−768.
(17) Ramakrishnan, N.; Clay, M. E.; Xue, L.-Y.; Evans, H. H.; Rodriguez-Antunez, A.; Oleinick, N. L. *Photochem. Photobiol.* **1988**, *48*, 297−303.
(18) Ortwerth, B. J.; Casserly, T. A.; Olesen, P. R. *Exp. Eye Res.* **1998**, *67*, 377−380.
(19) Au, V.; Madison, S. A. *Arch. Biochem. Biophys.* **2000**, *384*, 133−142.
(20) Michaeli, A.; Feitelson, J. *Photochem. Photobiol.* **1997**, *65*, 309−315.
(21) Foote, C. S.; Dobrowolski, D. C. In *Oxygen Radicals in Chemistry and Biology*; Bors, W., Saran, M., Tait, D., Eds.; Walter de Gruyter Co.: Berlin, New York, 1984; pp 465−472.
(22) Girotti, A. W. *Photochem. Photobiol.* **1990**, *51*, 497−509.
(23) Piette, J. *J. Photochem. Photobiol.* **1991**, *B*, 241−260.
(24) Cadet, J.; Teoule, R. *Photochem. Photobiol.* **1978**, *28*, 661−667.

HO_2^- [27] also shows no appreciable oxidative effect on purine and pyrimidine nucleosides at neutral pH.

Studies of the reactivity of DNA and its components with the primary radical species from the radiolysis of water ($e_{aq}^{\bullet -}$, $H^{\bullet}$, and $^{\bullet}OH$) and the secondary radicals produced from their reaction with organic or inorganic molecules have indicated that both pyrimidine and purine bases have a very high reactivity with $^{\bullet}OH$ (rate constants 10^9-10^{10} M^{-1} s^{-1}).[28] The $^{\bullet}OH$ reacts with not only purine or pyrimidine bases but also the deoxyribose unit, and these reactions usually lead to DNA chain breaks.

Singlet oxygen ($O_2{}^1\Delta_g$) is another reactive oxygen species of particular interest in biological systems because it can diffuse an appreciable distance. For example, in stearate monolayers, the distance for singlet oxygen half-deactivation was estimated to be 115 Å.[29] Singlet oxygen has been shown to be electrophilic, and therefore should be most reactive toward substrates with high electron-donating ability. The formation of singlet oxygen in biological systems may occur via photosensitization by the so-called Type II mechanism[30] or by chemical excitation by a number of pathways.[31−33] Type I, electron or hydrogen atom transfer, reactions can also occur in these systems, although we rule them out in this study.

The reactivities of nucleic acid bases with a variety of electrophilic reagents have been studied.[23] Both experiments and calculations have shown that guanine is the most reactive base with singlet oxygen.[34,35] These facts may explain the selective destruction of the guanine residue during photodynamic action.[23]

Although the photosensitized oxidation of guanosine and its derivatives has been extensively studied, the mechanism and the details of the chemical transformations involved are still not well understood. The main obstacles are the extremely low solubility of guanine and guanosine derivatives in most solvents, the instability of the primary products, and the complexity of the products formed, which often reflect substantial degradation.

In one of the few studies that has led to characterization of photooxidation products that are not extensively degraded, two main photooxidation products from the singlet oxygenation of 3′,5′-di-O-acetyl-2′-deoxyguanosine were reported to be the 4*R** and 4*S** diastereomers of 9-(3′,5′-di-O-acetyl-2′-deoxy-D-erythro-pentofuranosyl)-4,8-dihydro-4-hydroxy-8-oxoguanine,[24,36−38] formed from unstable diastereomeric intermediate endoperoxides from 1,4-cycloaddition of $^1O_2$.[38] However, it has recently been shown that these compounds are actually the diastereomeric spiroiminodihydantoins.[39−41]

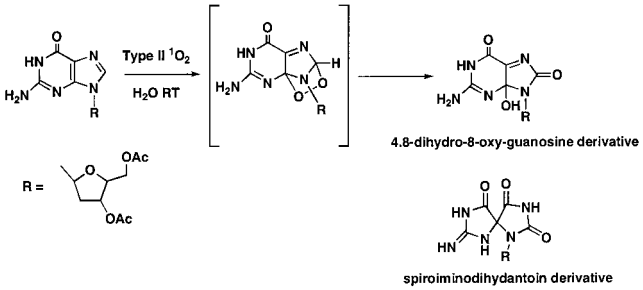

In our previous study of the low-temperature photooxidation of 2′,3′,5′-*O*-(*tert*-butyldimethylsilyl)-8-methylguanosine, we characterized an unstable endoperoxide as the primary intermediate.[42] We also characterized dioxetanes as primary intermediates and their unprecedented rearrangement to hydroperoxide intermediates in the photosensitized oxygenation of an organic-soluble 8-oxo-7,8-dihydroguanosine derivative by low-temperature NMR spectroscopy.[43] However, neither the endoperoxide nor the dioxetane intermediate has been directly observed in a native purine. In this paper, an organic-soluble guanosine derivative, 2′,3′,5′-*O*-(*tert*-butyldimethylsilyl)guanosine (**1**), is prepared and used as a model compound for low-temperature studies in an attempt to detect unstable intermediates and early decomposition products.

Results

Synthesis of Organic-Soluble Guanosine Derivatives. Several guanine, guanosine, and 2′-deoxyguanosine derivatives were synthesized to test their solubility in organic solvents (Supporting Information). The solvents used for solubility tests were those readily available deuterated and suitable for low-temperature NMR experiments. To prevent possible reactions with primary products, nucleophilic solvents such as methanol were avoided. For the purpose of easy spectrometer shimming, viscous solvents were also avoided. These considerations led to use of deuterated acetone-d_6, methylene chloride-d_2, and Freon-11.

The best derivative found, and the one used in this study, is 2′,3′,5′-*O*-(*tert*-butyldimethylsilyl)guanosine, **1**. This derivative is fully soluble in most organic solvents and allowed low-temperature experiments and characterization of unstable products. Also, the proton absorptions of the three *tert*-butyl and six methyl protecting groups are all at different chemical shifts, which reduces the NMR dynamic range problem and allows easier detection of the C(8)−H absorption in the guanine moiety. Another advantage of using this derivative is that the carbon absorptions of the protecting groups are all well separated from key purine resonance, which also helps in identifying the reaction products.

Photooxidation of 2′,3′,5′-*O*-(*tert*-Butyldimethylsilyl)guanosine (1). A solution of 2′,3′,5′-*O*-(*tert*-butyldimethylsilyl)-guanosine (**1**) and tetraphenylporphine (TPP) or 2,9,16,23-tetra-*tert*-butyl-29*H*,31*H*-phthalocyanine in CD_2Cl_2 was irradiated at 0 °C, room temperature, or −78 °C. Oxygen was continuously bubbled through the solution during the photolysis. A small amount of DMF was added as internal standard. The reaction

(25) Morgan, A. R.; Cone, R. L.; Elgert, T. M. *Nucleic Acid Res.* **1976**, *3*, 1139−1149.
(26) Loman, H.; Eber, M. *Int. J. Radiat. Biol.* **1970**, *18*, 369−379.
(27) Bielski, B. H.; Allen, A. O. *J. Phys. Chem.* **1977**, *81*, 1048−1050.
(28) Steenken, S. *Chem. Rev.* **1989**, *89*, 503−520.
(29) Schnuriger, B.; Bourdon, J. *Photochem. Photobiol.* **1968**, *8*, 361.
(30) Foote, C. S. *Photochem. Photobiol.* **1991**, *54*, 659−659.
(31) Russell, G. A. *J. Am. Chem. Soc.* **1957**, *79*, 3871.
(32) Cadenas, E.; Sies, H.; Nastainczyk, W.; Ullrich, V. *Z. Physiol. Chem.* **1983**, *364*, 519−528.
(33) Martinez, G. R.; Ravanat, J. L.; Medeiros, M. H. G.; Cadet, J.; Di Mascio, P. *J. Am. Chem. Soc.* **2000**, *122*, 10212−10213.
(34) Prat, F.; Hou, C. C.; Foote, C. S. *J. Am. Chem. Soc.* **1997**, *119*, 5051−5052.
(35) Saito, I.; Takayama, M.; Sugiyama, H.; Nakatani, K. *J. Am. Chem. Soc.* **1995**, *117*, 6406−6407.
(36) Cadet, J.; Decarroz, C.; Wang, S. Y.; Midden, W. R. *Israel J. Chem.* **1983**, *23*, 420−429.
(37) Cadet, J.; Berger, M.; Decarroz, C.; Wagner, J. R.; van Lier, J. E.; Ginot, Y. M.; Vigny, P. *Biochimie* **1986**, *68*, 813−834.
(38) Ravanat, J. L.; Cadet, J. *Chem. Res. Toxicol.* **1995**, *8*, 379−388.
(39) Niles, J. C.; Wishnok, J. S.; Tannenbaum, S. R. *Org. Lett.* **2001**, *3*, 963−966.
(40) Luo, W.; Muller, J. G.; Rachlin, E. M.; Burrows, C. J. *Org. Lett.* **2000**, *2*, 613−616.
(41) Adam, W. Personal communication, 2001.
(42) Sheu, C.; Foote, C. S. *J. Am. Chem. Soc.* **1993**, *115*, 10446−10447.
(43) Sheu, C.; Foote, C. S. *J. Am. Chem. Soc.* **1995**, *117*, 474−477.

Scheme 1

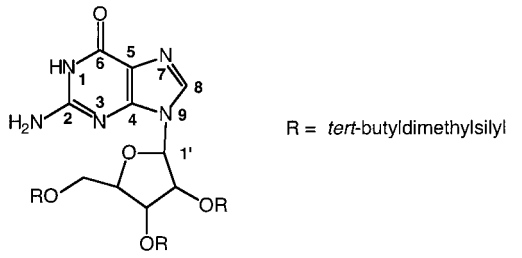

Scheme 2

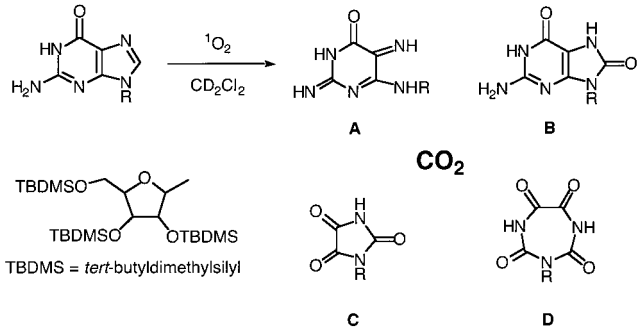

was monitored by NMR at various times. One major product, 6-[3,4-bis(*tert*-butyldimethylsilanyloxy)-5-(*tert*-butyldimethylsilanyloxymethyl)tetrahydrofuran-2-ylamino]-2,5-diimino-2,5-dihydro-3*H*-pyrimidin-4-one (**A**), and several minor ones (**B**−**D**, Scheme 2) were detected during the photolysis by observing the characteristic NMR C1′−H absorption peaks between 5.4 and 5.9 ppm. The C1′−H peak of the starting material at 5.83 ppm gradually disappeared as new products formed at 5.60 (**A**), 5.64 (**B**), 5.52 (**C**), and 5.45 ppm (**D**), respectively. Later experiments have shown that CO_2 was another major product and is derived from the C8 carbon.[44] The time course of the reaction is shown in Figure 1 and an expansion of the formation of compounds **B**−**D** is shown in Figure 2. Formation of parabanic acid C and its mechanism have been previously reported.[43]

When the photolyses were carried out in protiated instead of deuterated solvents, only a small amount of the above products were detected with the same irradiation time and intensity. This result is consistent with the well-known solvent deuterium isotope effect, which leads to an increase in the yields of products of singlet oxygen-mediated oxidation as a result of the increase in singlet oxygen lifetime.[45−47] The effects of adding singlet oxygen and radical scavengers during the photolysis are shown in Figure 3. The addition of 2,6-di-*tert*-butylphenol (DBP), a radical scavenger, did not cause any significant change in the reaction course. The slight decrease in the reaction rate is consistent with the small amount of quenching of singlet oxygen by DBP.[48] This result indicates that radical chains are not involved in the reaction. However, the addition of 1,4-diazabicyclo[2,2,2]octane (DABCO), a well-known singlet oxygen quencher, significantly decreased the disappearance rate of the starting material. This result and the solvent deuterium isotope effects support the view that singlet oxygen is the reactive oxidizing agent responsible for this reaction.

Very similar results were obtained when the reactions were carried out in acetone-d_6 at different temperatures with TPP or Rose Bengal as sensitizer. Neither an endoperoxide nor a dioxetane intermediate was detected even at −78 °C. The reaction is faster in solvents such as acetone-d_6 or acetonitrile-d_3 than in less polar solvents. When the reactions were performed at different temperatures in methylene chloride-d_2 or acetone-d_6, compound **A** was the only major product detected by NMR spectroscopy in all cases. The yields of **A** are dependent upon temperature and solvent; the results are sum-

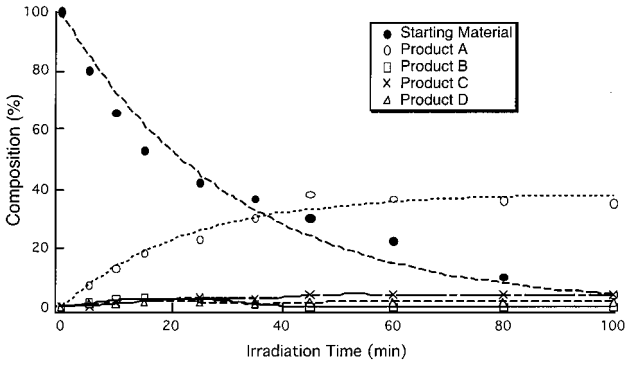

Figure 1. Time course of photooxidation of compound **1** at 0 °C (0.01 M **1** in CD_2Cl_2, 5×10^{-5} M TPP as sensitizer).

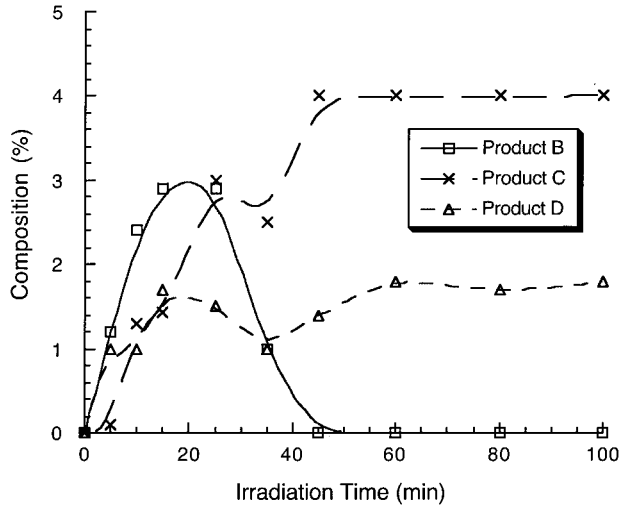

Figure 2. Time course of formation of products **B**−**D** in the photooxidation of compound **1** at 0 °C (0.01 M **1** in CD_2Cl_2, 5×10^{-5} M TPP as sensitizer; expansion of Figure 1).

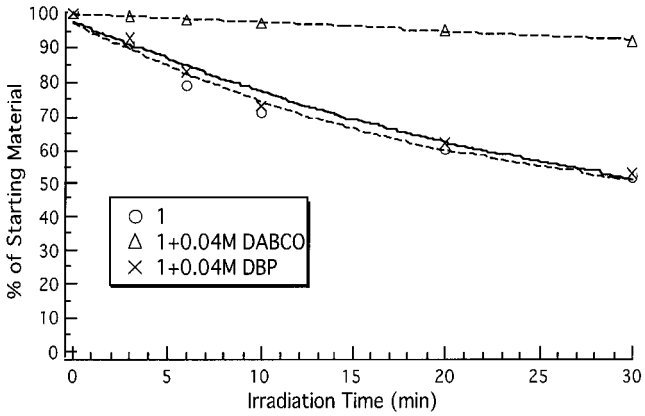

Figure 3. Additive effects in the photosensitized oxidation of 0.01 M **1** (○, **1**; △, **1** + 0.04 M DABCO; ×, **1** + 0.04 M DBP; 0 °C in CD_2Cl_2, 5×10^{-5} M TPP as sensitizer).

(44) Kang, P.; Foote, C. S. Submitted for publication, 2001.
(45) Ogilby, P. R.; Foote, C. S. *J. Am. Chem. Soc.* **1981**, *103*, 1219−1221.
(46) Ogilby, P. R.; Foote, C. S. *J. Am. Chem. Soc.* **1982**, *104*, 2069−2070.
(47) Ogilby, P. R.; Foote, C. S. *J. Am. Chem. Soc.* **1983**, *105*, 3423−3430.
(48) Thomas, M. J.; Foote, C. S. *Photochem. Photobiol.* **1978**, *27*, 683−693.

Table 1. Yields of Product **A** in the Photooxidation of 0.01 M Compound **1** in Methylene Chloride-d_2 and Acetone-d_6 at Different Temperatures

	product yields (%) (irradiation time, h)[a]	
T (°C)	CD_2Cl_2	$(CD_3)_2C{=}O$
22	19 (1.2)	13 (0.75)
0	36 (1.8)	28 (1.1)
−41	55 (3.5)	*b*
−78	61 (7.4)	54 (4.2)

[a] 5×10^{-5} M TPP as sensitizer. [b] Not determined.

Scheme 3

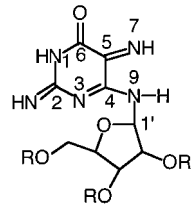

A

marized in Table 1. Mass balances are relatively poor in many of these reactions; in addition to compounds **B**−**D**, other uncharacterized materials are also formed.

Structure Determinations. Low-temperature (0 °C) column chromatographic purification gave **A** as the only major product; its structure was determined by spectroscopic data (see below). Product **B** was identified by spectral data and by comparison with an independently synthesized authentic sample.[43] Products **C** and **D** were found to be photoproducts of **B** and their structures were identified by comparison with the products of independent photosensitized oxidation of **B**.[43]

The structure of product **A** is assigned as the imidazole ring-opened product (6-[3,4,5-tris-(*tert*-butyldimethylsilanyloxy)-tetrahydrofuran-2-ylamino]-2,5-diimino-2,5-dihydro-3*H*-pyrimidin-4-one) shown in Scheme 3. The ^{1}H NMR spectrum of product **A** (in a mixture of guanosine and product **A**) in CD_2Cl_2 showed that the characteristic C8−H peak of starting material (**1**) at 7.97 ppm decreased as the reaction progressed and a new doublet at 7.65 ppm ($J = 8.7$ Hz) appeared. This peak disappeared upon adding CD_3OD and was assigned to the N9−H absorption. The C1′−H of the product appears in the NMR as a doublet of doublets (in acetone-d_6 5.75 ppm, $J_1 = 8.6$ Hz, $J_2 = 3.4$ Hz; it is a doublet in the starting material). Upon adding CD_3OD, the C1′−H peak coalesces to a doublet (5.75 ppm, $J = 4.0$ Hz). A COSY spectrum showed a strong cross-peak between the N(9) peak and C1′−H. The coupling between these two protons was also confirmed by homonuclear decoupling experiments. Since the starting material has no cross-peak between the C1′−H and the guanine moiety, this cross-peak indicates that a rearrangement of the guanine moiety occurred. The ^{1}H absorption of N7−H (12.10 ppm) is a sharp peak and does not change with solvent, which indicates no appreciable proton exchange between N7−H and other proton sources on the NMR time scale. There are two broad NH peaks in the ^{1}H NMR of product **A**: C2−NH at 10.34 ppm and N1−H at 6.32 ppm (this proton has a similar chemical shift as N1−H_2 of the starting material (6.63 ppm), probably from a tautomer that has an NH_2 group) in CD_2Cl_2. Both chemical shifts change with solvent. In acetone-d_6, the two NH peaks move upfield and closer (C2−NH at 7.45 ppm, N1−H at 6.51 ppm). We also observed that the higher the reaction conversion, the nearer to each other the two NH peaks are in CD_2Cl_2. This is probably due to the fact that the two NHs exchange protons with each other more rapidly in acetone-d_6 and may also exchange protons with residual water in acetone-d_6. The guanidine-like structure may promote the proton shuffling between N1 and C2−N, whereas N9 and N7 do not have appreciable intramolecular proton shifts. All the NH signals disappeared when CD_3OD was added.

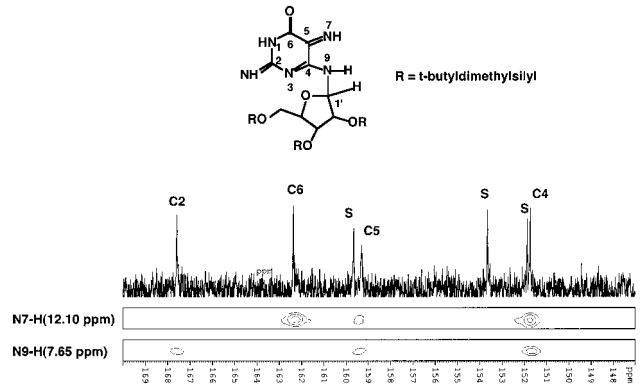

Figure 4. ^{1}H−^{13}C HMBC of the product **A**.

The ^{1}H−^{13}C HMBC spectrum of **A** confirms the structure assignment (Figure 4). The N7−H is coupled with C5 (159.30 ppm), C6 (162.37 ppm), and C4 (151.75 ppm). The N9−H is coupled with C4, C5, and C2 (167.60 ppm). A four-bond C−H coupling exists between N9−H and C2 but not between N9−H and C6. This may be due to the hydrogen bonding N9−H−N7 that results in a W configuration for C2−N3−C4−N9 (Figure 4). ^{1}H−^{13}C HMBC also confirmed the assignment of C1′−H (5.60 ppm), which has long-range C−H couplings with C2′, C3′, and C4′.

The ^{13}C NMR also showed similar carbon absorptions in the sugar region to those in the starting material. These similarities indicate that the sugar remains intact during the photolysis. This result is consistent with reports that the guanine base is more sensitive to photodynamic action than the ribose units.[49−52] The ^{13}C NMR spectrum for product **A** taken at −20 °C showed only nine carbon peaks (four for the base and five for the sugar).

An electrospray mass spectrum of the reaction mixture showed that the product has a molecular weight of 614.3 ([M + H]$^+$), 12 atomic units less than that of starting material (+O_2 − CO_2). The isolated mass spectrum of the product **A** was obtained by the MS-MS method. Some key features of the mass spectrum are fragments at *m*/*z* 445.1, 343.1, 308.3, 199.1, 152.0, 115.1, 89.0, and 73.1. A high-resolution electrospray MS spectrum showed the product has a molecular weight of 614.3562 ([M + H]$^+$, calculated 614.3589). These results and the formation of CO_2 from the C8[44] carbon strongly suggest that a carbon atom is missing after the photolysis. On the basis of these spectroscopic data, the structure of product **A** is assigned as the imidazole ring-opened product.

Direct Determination of $^1O_2$ Rate Constants ($k_q + k_r$) for Substrates. The total quenching (sum of physical (k_q) and

(49) Hallett, F. R.; Hallett, B. P.; Snipes, W. *Biophys. J.* **1970**, *10*, 305−315.
(50) Sastry, K. S.; Gordon, M. P. *Biochim. Biophys. Acta* **1966**, *129*, 42−48.
(51) Simon, M. I.; Van Vunakis, H. *J. Mol. Biol.* **1962**, *4*, 488−499.
(52) Sussenbach, J. S.; Berends, W. *Biochim. Biophys. Acta* **1965**, *95*, 184−185.

Table 2. Rates of Total Quenching ($k_r + k_q$) and Chemical Reaction (k_r) of Substrates with $^1O_2$ in Acetone-d_6

substrate	$(k_r + k_q)^a$ (10^{-6} M^{-1} s^{-1})	k_r (10^{-5} M^{-1} s^{-1})	rel k_r
1	6.33[b]	1.36[d]	1.0
A	nd	<0.013[e]	<0.01
B	55.4[b]	192[f]	141
CCO	0.013[c]		
TME	30.0[b]		
2M2P	0.76[b]		

[a] From decay of $^1O_2$ luminescence. [b] Reference 64. [c] Reference 65. [d] By competition with 2M2P, 2-Methyl-2-pentene (2M2P), *cis*-cyclooctene (CCO), and tetramethylethylene (TME). [e] By competition with CCO. [f] By competition with TME.

chemical (k_r) quenching) rate constants with $^1O_2$ were measured by directly observing the effect of added substrate on the observed decay rate of $^1O_2$ by following its luminescence at 1270 nm.[46] The slope of the plot of the observed rate of $^1O_2$ quenching vs substrate concentration is the total quenching rate constant of the substrate (Table 2).

Separation of Chemical Quenching (k_r) from Physical Quenching (k_q). Relative values of k_r can be measured by competition experiments. 2-Methyl-2-pentene (2M2P) and tetramethylethylene (TME) were chosen for these experiments because their reactions with $^1O_2$ have been intensely studied; since they do not quench $^1O_2$ appreciably, their ($k_r + k_q$) and k_r values are nearly identical,[53,54] and ($k_r + k_q$) $\sim k_r$ values of TME and 2M2P were determined by direct measurements with the laser apparatus. Reaction rates (k_r) of substrates were determined by competition experiments with the olefin of comparable reactivity.

The k_r value for **1** was determined by competition with 2-methyl-2-pentene (2M2P), for **A** by competition with *cis*-cyclooctene (CCO), and for **B** by competition with tetramethylethylene (TME). In all cases, the relative rate constants were determined by measuring the relative rate of appearance of the products or disappearance of the starting materials at low conversion (<20%). The disappearance of starting materials was monitored by NMR and the results were fit to the equation of Higgins et al.[55] k_r values for these substrates are also shown in Table 2.

Reaction of 1 with 4-Methyl-1,2,4-triazoline-3,5-dione and 4-Phenyl-1,2,4-triazoline-3,5-dione. Although the endoperoxide and dioxetane have been proposed as reaction intermediates,[36,42,43] we were unable to detect them by low-temperature NMR spectroscopy in this study. These intermediates may be too reactive to build up in the reaction even at the lowest temperature accessible. 4-Methyl-1,2,4-triazoline-3,5-dione (MTAD) and 4-phenyl-1,2,4-triazoline-3,5-dione (PTAD) are extremely reactive dienophiles and show behavior similar to singlet oxygen.[56−59] Reactions of **1** with 4-methyl-1,2,4-triazoline-3,5-dione (MTAD) and 4-phenyl-1,2,4-triazoline-3,5-dione (PTAD) were used as models for the singlet oxygen reaction;

Scheme 4

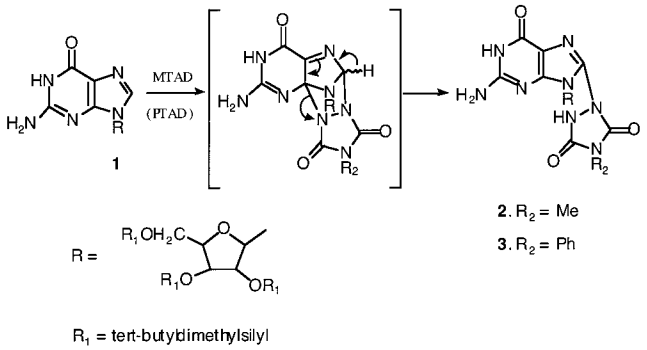

we sought products analogous to the endoperoxides and their possible rearrangement to hydroperoxide analogues (Scheme 4).

When the reaction of MTAD with **1** was carried out in CD_2Cl_2 and monitored by NMR spectroscopy, the intensity of the C8−H resonance peak at 8.04 ppm gradually decreased and a small peak at 7.97 ppm formed but did not build up during the reaction. We assign this to an unstable [4+2] adduct, the analogue of the endoperoxide. Presumably a subsequent rapid ring-opening of this cycloadduct gives **2** as the final product. Similar results were observed with 4-phenyl-1,2,4-triazoline-3,5-dione (PTAD) as the dienophile. The reactions were very slow at −78 °C. At room temperature, MTAD or PTAD reacted with **1** quantitatively to form the rearranged adducts within a few minutes. The products were isolated as white crystalline solids by slow crystallization from CH_2Cl_2 at −20 °C over a period of several days and then recrystallized from acetonitrile to give needlelike crystals. The structure of these adducts was determined by their ^{1}H NMR, ^{13}C NMR spectra, and X-ray crystal structure (in the case of the *N*-methyl compound, **2**, Figure 5).

Only one unstable [4+2] adduct intermediate was observed, since only one new MTAD methyl resonance was observed at 3.17 ppm. The X-ray crystal structure (Figure 5) of product **2** clearly indicated that the TBDMS protecting group at the C2′ position blocks one side of the imidazole ring of the guanine. Therefore, only one side is open for the approach of MTAD to form the [4+2] cycloadduct as primary intermediate. Based on these results, we suggest that the initial product for this reaction is the [4+2] cycloadduct. Because the C8−H in this adduct is labile, proton transfer from C8 to nitrogen yields **2** and **3** as final stable products (Scheme 4).

Discussion

Reactions of **1** with singlet oxygen in CD_2Cl_2 at various temperatures gave one major (**A**) and three minor (**B**−**D**) products. Neither an endoperoxide nor a dioxetane intermediate was observed by NMR spectroscopy even with reaction temperatures as low as −78 °C. Very similar results were obtained when the reactions were carried out in acetone-d_6. Several attempts to crystallize **A** or to make a stable derivative for X-ray structure determination failed, presumably because of the instability of the glycosidic linkage of this product. Indeed, both the hydrolytic scission of the glycosidic linkage and the rapid interconversion of the isomeric furanose and pyranose ribosides have been reported in 2,6-diamino-4-hydroxy-5-formamidopyrimidine.[60]

The base part of product **A** contains several imine functional groups and is also expected to be unstable under the reaction

(53) Manring, L. E.; Foote, C. S. *J. Am. Chem. Soc.* **1983**, *105*, 4710−4717.
(54) Sheu, C.; Foote, C. S.; Gu, C.-L. *J. Am. Chem. Soc.* **1992**, *114*, 3015−3021.
(55) Higgins, R.; Foote, C. S.; Cheng, H. *ACS Adv. Chem. Ser.* **1968**, *77*, 102.
(56) Smonou, I.; Orfanopoulos, M.; Foote, C. S. *Tetrahedron Lett.* **1988**, *29*, 2769−2772.
(57) Orfanopoulos, M.; Foote, C. S.; Smonou, I. *Tetrahedron Lett.* **1987**, *28*, 15−18.
(58) Jensen, F.; Foote, C. S. *J. Am. Chem. Soc.* **1987**, *109*, 6376−6385.
(59) Clennan, E. L.; Earlywine, A. D. *J. Am. Chem. Soc.* **1987**, *109*, 7104−7110.

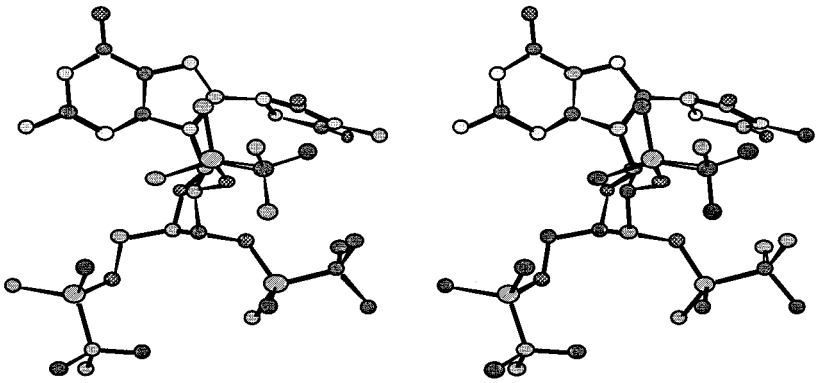

Figure 5. Stereoview (cross-eyed) of compound **2** (hydrogen atoms not shown).

Scheme 5

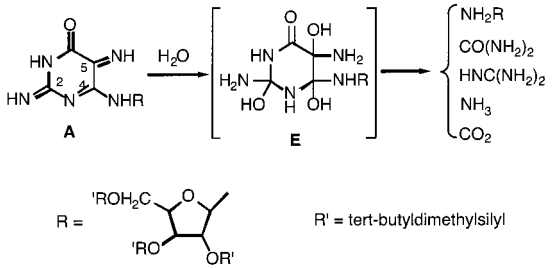

conditions. These imines may hydrolyze rapidly to generate compound **E**, which may further decompose to form ammonia, carbon dioxide, urea, and guanidine, etc., as final degradation products (Scheme 5).[52] The products and their distributions are complicated and may vary with the reaction conditions.

Imidazole ring-opening in the guanine moiety has been reported in several cases, such as the base hydrolysis of 7-methylguanine[61] and on treatment of 2′-deoxyguanosine with mitomycin.[60] Recently, formation of an imidazole ring-opened product has also been reported by Gajewski et al.[62] Their results showed that a 2,6-diamino-4-hydroxy-5-formamidopyrimidine (FapyGua) was formed in both γ-irradiated and visible light/MB-treated DNA and is recognized and excised by the Fpg protein. Although the 2,6-diamino-4-hydroxy-5-formamidopyrimidine was suggested to be a $^1O_2$ reaction product, no mechanistic data for formation of this product were provided and it could also be explained by the one-electron oxidation mechanism.

In the present study, we have shown that this ring-opened product has structure **A** and is the major product in the photosensitized oxidation of these guanosine derivatives in various solvents. Our results indicate that there is no significant time delay (Figure 1) in the formation of product **A** at room temperature. Thus, either **A** is the primary product or, more probably, the primary intermediate which leads to the formation of **A** is much more unstable and does not build up. Work under review has identified intermediates preceding A.[44]

The mechanism for the formation of product **A** on reaction with $^1O_2$ is still uncertain. The most likely process is the [4+2] cycloaddition of singlet oxygen to the imidazole ring of the guanine base to form an endoperoxide as primary intermediate. Proton transfer with subsequent rearrangement of the corresponding allylic hydroperoxide would give **A** as the final oxidative product (Scheme 6).

Scheme 6

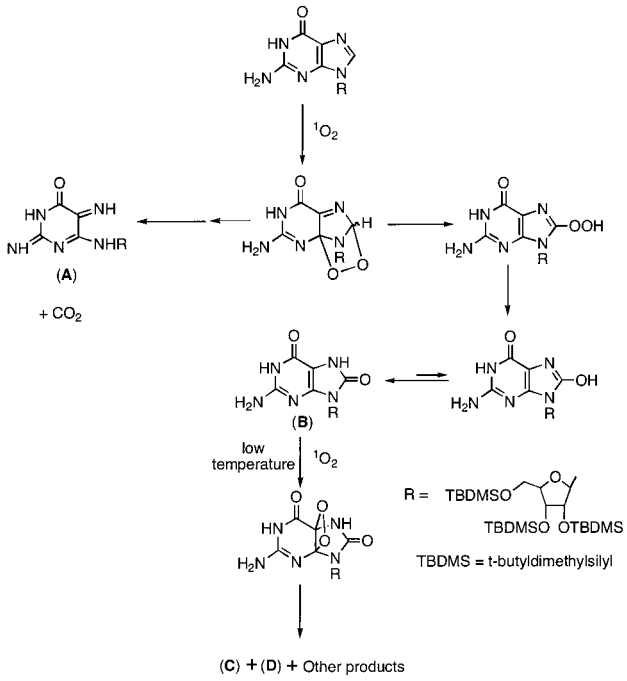

However, if this is the only process occurring, the yield of product **A** should remain nearly constant or decrease with longer irradiation time. However, from Table 1, the irradiation time required for total conversion of the starting material is longer at lower temperatures but higher yields of **A** are obtained. In addition, this mechanism alone would not account for the formation of products **B**−**D**. Probably, other processes compete at higher temperatures.

Competition experiments in Table 2 indicated that **A** is about 2 orders of magnitude less reactive than **1**. The low yields of **A** at higher temperatures may result from hydrolytic or other degradation of **A** at higher temperatures, but further reaction of **A** with $^1O_2$ can be neglected.

To account for the formation of other products, an alternative mechanism (Scheme 6) that involves the formation of 8-hydroxyguanosine and its more stable keto form, 8-oxo-7,8-dihydroguanosine, is proposed. In this mechanism, a very reactive

(60) Tomasz, M.; Lipman, R.; Lee, M. S.; Verdine, G. L.; Nakanishi, K. *Biochemistry* **1987**, *26*, 2010−2027.
(61) Brookes, P.; Lawley, P. D. *J. Chem. Soc.* **1961**, 3923−3928.
(62) Boiteux, S.; Gajewski, E.; Laval, J.; Dizdaroglu, M. *Biochemistry* **1992**, *31*, 106−110.

8-hydroperoxy derivative is formed by rearrangement of the initial endoperoxide through the hydrogen transfer from the C-8 position to oxygen atom. The driving force for ring opening is relief of ring strain and regaining aromaticity.

Support for this mechanism comes from the reactions of PTAD or MTAD with **1**. Reactions of PTAD or MTAD with **1** failed to produce the corresponding [4+2] cycloadducts as stable products (although transient intermediate adducts were detected by NMR). Instead, compounds **2** and **3**, which are analogous to hydroperoxides, were obtained. This result explains our inability to observe the endoperoxide during the photosensitized oxidation of **1** by low-temperature (−78 °C) NMR spectroscopy since the endoperoxide is probably even less stable and should open to the hydroperoxide.

The hydroperoxide (an iminoperacid) can probably oxidize other substrates including the starting guanosine and be reduced to 8-hydroxyguanosine. Since 8-hydroxyguanosine tautomerizes to the more stable keto form at room temperature, its reactivity toward singlet oxygen is not measurable. However, its reactivity would be expected to be similar to that of 8-methoxyguanosine, which is about 8 times as reactive as the starting material.[63]

More likely, the 8-hydroxyguanosine tautomerizes to the more stable keto form (compound **B**). The 8-oxo compound **B** is formed in small amounts, and was identified by comparison with an authentic sample. Competition experiments showed that **B** is 2 orders of magnitude more reactive than **1**[64] and is therefore too reactive to build up in the reaction mixture, consistent with the fact that **B** is only observed during the initial stage of photooxidation (Figure 2) and its maximum yield is less than 3.5%. We have already shown that reaction of compound **B** with singlet oxygen gives dioxetanes and hydroperoxides as primary intermediates which decompose to provide **C**, **D**, and other compounds as final products.[43]

Conclusion

The reaction of singlet oxygen with an organic-soluble guanosine derivative causes opening of the imidazole ring to give **A** as the major product. The yields of this product depend on the reaction conditions. Although no endoperoxide or dioxetane intermediate was observed by low-temperature NMR spectroscopy even down to −78 °C, a mechanism involving initial [4+2] cycloaddition of singlet oxygen with the imidazole ring to form an unstable endoperoxide is proposed to account for these results. This endoperoxide undergoes subsequent proton transfer to form the hydroperoxide (8-hydroperoxyguanosine), which can be reduced to 8-hydroxyguanosine and in turn is converted to the stable keto form and reacts with singlet oxygen to give the final products. The formation of the 8-hydroperoxyguanosine as reactive intermediate is supported by reactions of this guanosine derivative with MTAD or PTAD to give an analogous product.

Experimental Section

General. ^{1}H and ^{1}C NMR spectra were recorded on Bruker AF-200, AM-360, ARX-500, and Avance 500 spectrometers. ^{13}C NMR spectra were taken with the solvent as reference. Chemical shift values are in ppm downfield from internal tetramethylsilane in the indicated solvent. ^{13}C NMR peak multiplicity was determined by DEPT experiments. Infrared spectra were taken on Perkin-Elmer PE 580 and 1600 instruments. Samples were prepared either neat on NaCl plates or as KBr pellets. Thin-layer chromatograms were obtained with either DC-Fertigplatten Kieselgel 60 F254 or DC-Plastikfolien Kieselgel 60 F254 from E. Merck. Column chromatography was performed on silica gel 60, 70−230 mesh or 230−400 mesh (flash column) from E. Merck, and on neutral alumina, activity I, from Fisher.

Materials. Fe_2SO_4, Na_2SO_4, KOH, glacial acetic acid, and Florisil were from Fisher, and NaH was from Alfa. All other compounds were from Aldrich and were used as received. To prepare dry guanosine, guanosine hydrate was heated over P_2O_5 in a vacuum at 56 °C for 3 h before use. Commercial solvents were Fisher AR, used without further purification. Deuterated solvents were from Cambridge Isotope Laboratory and were dried over 4 Å Molecular Sieve before use. Anhydrous *N*,*N*-dimethylformamide (DMF) was prepared by stirring DMF with CaH_2 (5 g/L) overnight at room temperature and distilled under reduced pressure (bp 70−80 °C, 20−30 mmHg).

Preparation of 2′,3′,5′-*O*-(*tert*-Butyldimethylsilyloxy)guanosine. To a solution of guanosine (5.6 g, 20 mmol) and imidazole (13.6 g, 200 mmol) in 50 mL of anhydrous DMF was added 15.0 g (100 mmol) of *tert*-butyldimethylsilyl chloride (TBDMSCl). The reaction mixture was stirred at room temperature under N_2 for 26 h. The resulting mixture was poured into EtOAc−H_2O. The organic layer was dried over anhydrous Na_2SO_4 and evaporated. Column chromatographic purification (1:1 CH_2Cl_2/CH_3CN) gave 11.4 g (91%) of 2′,3′,5′-*O*-(*tert*-butyldimethylsilyloxy)guanosine, which was recrystallized from 95% EtOH to give white needles, mp >300 °C dec. ^{1}H NMR (CD_2Cl_2, δ 5.32 ppm) 12.30 (s, 1H, N1−H), 7.97 (s, 1H, C8−H), 6.63 (s, br, 2H, C2−NH_2), 5.83 (d, J = 3.9 Hz, 1H, C1′−H), 4.44 (dd, J = 4.0 Hz, 3.9 Hz, C2′−H), 4.32 (dd, J = 4.3 Hz, 4.0 Hz, 1H, C3′−H), 4.11 (ddd, J = 4.3 Hz, 3.3 Hz, 2.3 Hz, 1H, C4′−H), 4.02 (dd, J = 11.6 Hz, 3.3 Hz, 1H, C5′−H″), 3.82 (dd, J = 11.6 Hz, 2.3 Hz, 1H, C5′−H′), 0.99, 0.94, 0.89 (s, 27H, 3 × *tert*-butyl), 0.17, 0.16, 0.13, 0.11, 0.06, 0.03 (s, 18H, 6 × Me). ^{13}C NMR (CD_2Cl_2, δ 53.8 ppm) 154.4 (s, C2), 151.6(s, C4), 117.6 (s, C5), 159.5 (s, C6), 135.9 (d, C8), 88.7 (d, C1′), 76.9 (d, C2′), 71.5 (d, C3′), 85.0 (d, C4′), 62.5 (t, C5′, 26.3, 26.0, 25.9 (q, 3 × C(CH_3)$_3$), 18.8, 18.3, 18.2, (s, 3 × C(CH_3)$_3$), −4.11, −4.52, −4.61, −4.65, −5.25, −5.28 (q, 6 × Me); IR (KBr, cm^{-1}) 3320, 3200, 2912, 2720, 1728, 1685, 1650, 1570, 1488, 1420, 1392, 1364, 1340, 1177, 1121, 1100, 1083, 1052, 777, 681.

Photooxidation of 2′,3′,5′-*O*-(*tert*-Butyldimethylsilyloxy)guanosine. A 12.6 mg (0.02 mmol) sample of 2′,3′,5′-*O*-(*tert*-butyldimethylsilyloxy)guanosine was dissolved in ca. 0.5 mL of CD_2Cl_2 in a 5-mm NMR tube with ca. 5 × 10^{-5} M of 5,10,15,20-tetraphenyl-21*H*,23*H*-porphine (TPP) or 2,9,16,23-tetra-*tert*-butyl-29*H*,31*H*-phthalocyanine as sensitizer and a Cermax 300-W Xenon lamp as the light source. A 1% potassium dichromate filter solution was used to cut off wavelengths below 500 nm and an 18 cm long water filter was placed in front of the sample tube to eliminate heating. When the photolysis was carried out at room temperature, the reaction was complete within a few hours. However, the yield of product was very low, presumably because of decomposition of the primary products. When the photooxidation was performed at −78 °C, the reaction was slower than at room temperature. The reaction was complete after 36 h irradiation and the product yield was much higher. The ^{1}H NMR spectrum of the reaction mixture at −78 °C was similar to that at −20 °C, 0 °C, and room temperature, except that the peaks were broad at lower temperature. Only one major product formed. Low-temperature (0 °C) column chromatographic purification with 100% hexane as eluent to remove TPP, then pure CH_2Cl_2, then 1:1 CH_2Cl_2/CH_3CN gave a product whose ^{1}H NMR spectrum is identical with that of the major product in the reaction mixture.

Product **A** (in the mixture of unreacted guanosine and **A**): ^{1}H NMR (−20 °C, CD_2Cl_2, δ 5.32 ppm) 12.10 (s, 1H, N1−H), 10.35 (s, br, 1H, C1−H), 7.65 (d, J = 7.0 Hz, 1H, N9−H), 6.32 (s, br, 1H, C2−NH),

(63) Sheu, C.; Foote, C. S. *J. Org. Chem.* **1995**, *60*, 4498−4503.
(64) Sheu, C.; Foote, C. S. *J. Am. Chem. Soc.* **1995**, *117*, 6439−6442.

5.60 (d, J = 6.4 Hz, 1H, C1′−H), 4.27 (dd, J = 5.1 Hz, 4.5 Hz, C3′−H), 4.08 (d, J = 2.1 Hz, 1H, C2′−H), 4.00 (d, J = 5.8 Hz, 1H, C4′−H), 3.84 (d, J = 10.4 Hz, 1H, C5′−H″), 3.66 (d, J = 11.0 Hz, 1H, C5′−H′), 0.96, 0.95, 0.82 (s, 27H, 3 × *tert*-butyl), 0.19, 0.15, 0.14, 0.13, 0.12, 0.11 (s, 18H, 6 × Me). ^{13}C NMR (−20 °C CD_2Cl_2, δ 53.8 ppm) 167.6 (s, C2), 162.4 (s, C6), 159.3 (s, C5), 151.7 (s, C4), 86.7 (s, C1′), 83.7 (s, C4′), 76.5 (s, C2′), 70.2 (s, C3′), 61.1 (s, C5′). This product is not stable in solution at room temperature and decomposes to a mixture of unknown products after standing at room temperature for 1 day. Similar results were obtained in acetone-d_6 at −78 °C with TPP, 2,9,16,23-tetra-*tert*-butyl-29*H*,31*H*-phthalocyanine, or Rose Bengal as sensitizer. ^{1}H NMR (−20 °C, acetone-d_6, δ 2.05 ppm) 12.13 (s, 1H, N1−H), 7.90 (d, J = 8.8 Hz, 1H, N9−H), 7.45 (s, br, 1H, N1−H), 6.51 (s, br, 1H, C2−N−H), 5.75 (dd, J = 8.7 Hz, 3.4 Hz, 1H, C1′−H). ^{13}C NMR (−20 °C acetone-d_6, δ 206.0 ppm) 167.7 (s, C2), 161.7 (s, C6), 159.9 (s, C5), 152.5 (s, C4), 86.1 (s, C1′), 83.3 (s, C4′), 76.3 (s, C2′), 70.9 (s, C3′), 61.3 (s, C5′).

Mass Spectra of Product A. Electrospray mass spectra of the reaction mixture were obtained on a PE SCIEX, API III Biomolecular Mass Analyzer. The MS of product **A** was measured on the parent peak of 614.3 by the MS-MS method. **A**: 614.3 $[M + H]^+$, 445.1, 343.1, 308.3, 266.0, 211.1, 199.1, 181.1, 152.0, 115.1, 89.0, 73.1. A high-resolution ESI spectrum was done on a FT-ICR-MS machine by Dr. Fei He of the National High Magnetic Field Laboratory, Florida State University. Product **A** had m/z 614.35624 $[M + H]^+$, within 4 ppm of the calculated value (614.35893 $[M + H]^+$).

Direct Determination of Singlet Oxygen Quenching Rate ($k_r + k_q$). The rates of interaction ($k_r + k_q$) of substrates with $^1O_2$ were determined in acetone-d_6 by time-resolved studies of singlet oxygen luminescence at 1270 nm. The apparatus was a modification of the one previously described.[47] Sensitizing dyes were excited with either the second (532 nm) or third (355 nm) harmonic of a Quanta-Ray (DCR-2) Nd:YAG laser. The laser pulse was filtered to remove any fundamental from the laser using a 355/532 nm pass/1060 nm reflecting mirror, followed with a Schott KG-3 infrared absorbing filter that removed any residual fundamental radiation. The 355 nm pulse was also filtered with a 355 nm pass/532 nm reflecting mirror. The near-infrared emission from $^1O_2$ was monitored at a right angle to the laser beam and filtered with Schott RG-850 and silicon 1100 nm (Infrared Optics) cutoff filters. The detector was a liquid N_2-cooled germanium photodiode (Model EO-817P, North Coast Scientific Corp.). The signal was averaged (10−12 shots) in a transient digitizer (LeCroy 9410), then transferred to a Macintosh IIci computer with Labview software. The data were analyzed by fitting with an exponential, using Igor graphics software and a macro written by Dr. R. Kanner.

Determination of the Rate conStant (k_r) of Reaction with Singlet Oxygen. The k_r values for compound **1**, **A**, and **B** were determined by competition with 2-methyl-2-pentene (2M2P), *cis*-cyclooctene (CCO), and tetramethylethylene (TME), respectively. In all cases, the relative rates were determined by measuring the relative appearance of the products or the disappearance of starting materials at low conversion (<20%) by NMR spectroscopy. Zero and first-order baseline corrections were applied before peak integration; a small amount of DMF was used as internal integration reference. The ($k_q + k_r$) values of 2M2P, CCO, and TME were determined by time-resolved singlet oxygen luminescence at 1270 nm and are 7.6×10^5, 1.3×10^4, and 3.0×10^7 M^{-1} s^{-1}, respectively.[64,65]

Reaction of 2′,3′,5′-*O*-(*tert*-Butyldimethylsilyloxy)guanosine with 4-Methyl-1,2,4-triazoline-3,5-dione. To a solution of 2′,3′,5′-*O*-(*tert*-butyldimethylsilyloxy)guanosine (62.8 mg, 0.10 mmol) in 5.0 mL of anhydrous CH_2Cl_2 at −78 °C was added dropwise 11.3 mg (0.10 mmol) of 4-methyl-1,2,4-triazoline-3,5-dione (MTAD) in 1 mL of anhydrous CH_2Cl_2. The reaction mixture was stirred at −78 °C for 20 min and then allowed to warm to room temperature; the pink color gradually disappeared. The resulting solution was kept at −20 °C overnight and the white precipitate was filtered and recrystallized from CH_3CN to give needles (**2**). The reaction is very fast at room temperature and gave the same results.

Product **2**: ^{1}H NMR (DMSO-d_6) δ 3.67 (d, J = 6.4 Hz, 2H, C5′−H), 3.84 (t, J = 6.4 Hz, 1H, C4′−H), 4.12 (d, J = 4.4 Hz, 1H, C3′−H), 5.15 (dd, J = 7.0 Hz, 4.4 Hz, 1H, C2′−H), 5.55 (d, J = 7.0 Hz, 1H, C1′−H), 6.51 (s, br, 2H, C2−NH_2), 2.98 (s, 3H, N−CH_3), 10.87 (s, br, 1H, N−H), 11.21 (s, br, 1H, N1−H), 0.87, 0.84, 0.77 (s, 27H, 3 × *tert*-butyl's), 0.08, 0.06, 0.02, 0.01, −0.12, −0.28 (s, 18H, 6 × Me). ^{13}C NMR (DMSO-d_6) δ 154.0 (s, C2), 151.3 (s, C4), 115.0 (s, C5), 156.2 (s, C6), 135.6 (d, C8), 86.7 (d, C1′), 72.9 (d, C2′), 71.7 (d, C3′), 85.5 (d, C4′), 62.6 (t, C5′), 153.5 (s, C═O), 153.3 (s, C═O), 25.1 (q, N−CH_3), 25.8, 25.7, 25.6 (q, 3 × C(CH_3)$_3$), 17.9, 17.7, 17.6, (s, 3 × C(CH_3)$_3$), −4.7, −4.7, −5.1, − 5.5, −5.5, −5.6 (q, 6 × Me).

Reaction of 2′,3′,5′-*O*-(*tert*-Butyldimethylsilyloxy)guanosine with 4-Phenyl-1,2,4-triazoline-3,5-dione. To a solution of 2′,3′,5′-*O*-(*tert*-butyldimethylsilyloxy)guanosine (62.8 mg, 0.10 mmol) and 5.0 mL of anhydrous CH_2Cl_2 at −78 °C was added dropwise 17.5 mg (0.10 mmol) of 4-phenyl-1,2,4-triazoline-3,5-dione (PTAD) in 1 mL of anhydrous CH_2Cl_2. The reaction was stirred at −78 °C for 20 min and then warmed to room temperature. The pink color gradually disappeared on warming. The resulting solution was kept in the freezer (−20 °C) overnight and the white precipitate was recrystallized from CH_3CN to give needles (**3**), mp >250 °C dec. The reaction is very fast at room temperature and gave the same results.

Product **3**: ^{1}H NMR (DMSO-d_6) δ 3.69 (dd, J = 10.4 Hz, 5.3 Hz, 1H, C5′−H′), 3.78 (dd, J = 10.4 Hz, 10.2 Hz, 1H, C5′−H″), 3.86 (dd, J = 10.4 Hz, 5.3 Hz, 1H, C4′−H), 4.17 (d, J = 4.4 Hz, 1H, C3′−H), 5.31 (dd, J = 7.0 Hz, 4.4 Hz, 1H, C2′−H), 5.59 (d, J = 7.0 Hz, 1H, C1′−H), 6.50 (s, br, 2H, C2−NH_2), 7.45−7.56 (m, 5H, C_6H_5), 10.91 (s, br, 1H, N−H), 11.70 (s, br, 1H, N(1)−H). ^{13}C NMR (DMSO-d_6) δ 154.0 (s, C2), 151.3 (s, C4), 115.2 (s, C5), 156.2 (s, C6), 135.2 (d, C8), 87.0 (d, C1′), 72.9 (d, C2′), 71.3 (d, C3′), 85.6 (d, C4′), 62.7 (t, C5′), 151.77 (s), 151.6 (s), 131.5, (s), 129.0 (d), 128.4 (s), 126.0 (d), 25.8, 25.7, 25.6 (q, 3 × C(CH_3)$_3$), 17.9, 17.7, 17.6, (s, 3 × C(CH_3)$_3$), −4.70, −4.71, −5.11, 5.37, −5.41, −5.50 (q, 6 × Me).

X-ray Crystal Structure of Compound 2. A crystal of approximate dimensions 0.30 × 0.10 × 0.05 mm^3 was glued to the tip of a glass fiber and mounted on a modified Picker four-circle diffractometer equipped with a gas-stream low-temperature device and graphite monochromatized Mo source. Accurate unit cell parameters and orientation matrix were obtained by a least-squares fit to the automatically centered settings of 20 reflections, and are given in the Supporting Information together with other details. The diffraction data were collected with a $\theta/2 - \theta$ scan mode up to a maximum $2 - \theta$ of 40° at low temperature (128 K).

The structure was solved in the orthorhombic space group *P*212121 by direct methods using SHELX86, which revealed the positions of all non-hydrogen atoms. This was followed by several cycles of full-matrix least-squares refinement. Hydrogen atoms were included as fixed contributors to the final refinement cycles. The positions of hydrogen atoms were calculated on the basis of idealized geometry and bond length (C−H = 1.00 Å). In the final cycles of least-squares refinement, all non-hydrogen atoms were refined with anisotropic thermal coefficients. Convergence resulted in final agreement factors of $R = 0.088$ and $R_w = 0.088$.

Acknowledgment. Supported by NIH grant no. GM-20081 and NSF grant no. CHE-9730386. We thank Dr. Kym F. Faull and Mr. Kenneth Conklin for their help in obtaining FAB-MS and low-resolution ESI spectra. We also thank Dr. Fei He, Dr.

(65) Poon, T. H. W.; Pringle, K.; Foote, C. S. *J. Am. Chem. Soc.* **1995**, *117*, 7611−7618.

Chris Hendrickson, and Dr. Mark Emmett of The National High Magnetic Field Laboratory, Tallahassee for measuring the high-resolution ESI of product **A.** NMR was supported by NSF CHE-9974928.

Supporting Information Available: Synthesis of organic-soluble guanosine derivatives; ^{1}H NMR and ^{13}C NMR spectra data for compound **A**; electrospray MS spectra of **A**; tables of crystal data, fractional atomic coordinates, isotropic and anisotropic parameters, bond distances and angles for **2**, and listing of observed and calculated structure factors (PDF). This material is available free of charge via the Internet at http://pubs.acs.org.

JA011696E